Development 129, 2555-2563 (2002)
Printed in Great Britain © The Company of Biologists Limited 2002
DEV5017

Delta-Notch signaling induces hypochord development in zebrafish

Andrew J. Latimer, Xinhong Dong, Youlia Markov and Bruce Appel*

Department of Biological Sciences, Vanderbilt University, Nashville, TN 37232, USA
*Author for correspondence (e-mail: b.appel@vanderbilt.edu)

Accepted 15 March 2002

SUMMARY

Different cell types that occupy the midline of vertebrate embryos originate within the Spemann-Mangold or gastrula organizer. One such cell type is hypochord, which lies ventral to notochord in anamniote embryos. We show that hypochord precursors arise from the lateral edges of the organizer in zebrafish. During gastrulation, hypochord precursors are closely associated with *no tail*-expressing midline precursors and paraxial mesoderm, which expresses *deltaC* and *deltaD*. Loss-of-function experiments revealed that *deltaC* and *deltaD* were required for *her4* expression in presumptive hypochord precursors and for hypochord development. Conversely, ectopic, unregulated Notch activity blocked *no tail* expression and promoted *her4* expression. We propose that Delta signaling from paraxial mesoderm diversifies midline cell fate by inducing a subset of neighboring midline precursors to develop as hypochord, rather than as notochord.

Key words: Delta, Notch, Notochord, Hypochord, Midline, Fate map, Zebrafish, Gastrulation

INTRODUCTION

During vertebrate development dorsally located cells, known as the gastrula or Spemann-Mangold organizer, provide a source of signals that induce embryonic axis formation. After gastrulation, cells that originated within the organizer occupy the midline of all three germ layers: floor plate of ventral neural tube, mesodermal notochord ventral to neural tube and dorsal endoderm (Spemann, 1938; Schoenwolf and Sheard, 1990; Selleck and Stern, 1991; Gont et al., 1993; Catala et al., 1996; Wilson and Beddington, 1996). Also at the midline of anamniote embryos, such as axolotls, frogs and fish, are hypochord cells, which form a single row directly ventral to notochord (Lofberg and Collazo, 1997; Cleaver et al., 2000; Eriksson and Lofberg, 2000). Midline cells are an important source of signals that pattern nearby tissues subsequent to axis formation. For example, notochord and floor plate secrete Sonic hedgehog (Shh), which patterns ventral neural tube and somites (Tanabe and Jessell, 1996; Stickney et al., 2000), and hypochord cells secrete VEGF, which appears to be required for dorsal aorta formation (Cleaver and Krieg, 1998). Thus, an important step toward understanding vertebrate development is understanding the mechanisms that specify midline cells.

In zebrafish, development of midline cells requires the Delta ligand-Notch receptor signaling system. Specifically, embryos with a mutation of *deltaA* (*dla*), one of four known zebrafish Delta homologs, have a deficit of floor-plate and hypochord cells and excess notochord cells; by contrast, overexpression of *dla* blocked notochord development and produced excess floor-plate and hypochord cells (Appel et al., 1999). Fate mapping had shown that notochord and floor-plate precursors are close together in the zebrafish organizer (Shih and Fraser, 1995; Melby et al., 1996) and functional analyses of *no tail* (*ntl*), which encodes a T-box transcription factor homologous to mouse Brachyury, had indicated that Ntl mediates a choice between notochord and floor-plate fates (Halpern et al., 1997). As gastrula stage zebrafish embryos express Delta and Notch genes (Bierkamp and Campos-Ortega, 1993; Dornseifer et al., 1997; Westin and Lardelli, 1997; Haddon et al., 1998; Appel et al., 1999), we hypothesized that Delta-Notch signaling during gastrulation regulates specification of zebrafish midline precursors for notochord, floor-plate and hypochord fates by regulating *ntl* expression.

We present tests of hypochord specification. By fate mapping, we found that hypochord precursors arise from the edge of the shield, which is the zebrafish gastrula organizer. These cells are closely associated with cells that become either notochord or slow muscle but not floor plate. Presumptive hypochord precursors express *notch5* and *her4*, a Notch target gene, during gastrulation. Initially, all *her4*-expressing cells express *ntl*, which marks midline precursors, but later they do not. This raises the possibility that hypochord precursors emerge from the *ntl*-positive midline precursor population. Cells that express *her4* are close to cells of the paraxial mesoderm, which express *deltaC* (*dlc*) and *deltaD* (*dld*), and loss-of-function experiments show that *dla*, *dld* and *dla*, which gastrulating embryos uniformly express, are redundantly required for *her4* expression and hypochord development. Finally, we show that unregulated Notch activity inhibits *ntl* expression. We propose that cells at the lateral edges of the midline precursor domain can develop either as notochord or hypochord, and that hypochord development is induced by Delta ligands expressed by neighboring paraxial mesoderm cells.

MATERIALS AND METHODS

Embryos

Embryos were collected from single pair matings and raised at 28.5°C in embryo medium (15 mM NaCl, 0.5 mM KCl, 1 mM $CaCl_2$, 1 mM $MgSO_4$, 0.15 mM KH_2PO_4, 0.05 mM NH_2PO_4, 0.7 mM $NaHCO_3$) and staged according to hours postfertilization (hpf) and morphological criteria (Kimmel et al., 1995). The *aei* mutant allele we used, originally designated aei^{tr233} (van Eeden et al., 1996) and redesignated aei^{AR33}, creates a stop codon within the fifth EGF-like repeat of *dld* (Holley et al., 2000).

Cell labeling

We injected one- to four-cell stage zebrafish embryos with a 2% solution of DMNB-caged fluorescein dextran (Molecular Probes) in 1× Danieau solution. Injected embryos were maintained in the dark at 28.5°C in embryo medium until shield stage. Embryos were dechorionated with watchmaker's forceps and mounted in 2% methyl cellulose on bridged slides with the dorsal side of the embryos facing upwards. The dye was photoactivated in three to five cells using 5-10 second pulses of 365 nm light (Serbedzija et al., 1998) generated by a Photonics Micropoint Laser System focused using a 40× objective mounted on a Zeiss Axiskop. Dye activation was confirmed using epifluorescence optics. Labeled embryos were maintained at 28.5°C until 24 hpf, at which time the fates of the labeled cells were determined by examining living embryos with a compound microscope. Images were obtained using a Hammamatsu Orca CCD camera. Embryos selected for histochemical analysis were fixed in 4% paraformaldehyde.

In situ RNA hybridization and immunohistochemistry

Previously described probes include those for *notch5* (Westin and Lardelli, 1997), *notch1a* (Bierkamp and Campos-Ortega, 1993), *her4* (Takke et al., 1999), *myod* (Weinberg et al., 1996), *ntl* (Schulte-Merker et al., 1994), *dld* and *dlc* (Haddon et al., 1998), *col2a1* (Yan et al., 1995), and *isl1* (Appel et al., 1995). In situ RNA hybridization was performed essentially as described (Hauptmann and Gerster, 2000; Jowett, 2001). For double labeling, best results were obtained by staining with BCIP/NBT (Roche Diagnostics) first, followed by staining with BCIP/INT (Roche Diagnostics). To convert the fluorescent signal in photoactivated embryos to a blue precipitate, the embryos were incubated with alkaline phosphatase-conjugated anti-fluorescein antibody (Roche Diagnostics) at 1:10,000 dilution followed by staining with BCIP/NBT. Slow muscle cells were detected by incubating embryos with monoclonal F59 antibody (gift of Frank Stockdale) at 1:10 dilution, followed by incubation with Alexa Fluor 568 goat anti-mouse IgG conjugate (Molecular Probes) at 1:200 dilution. Myc expression was detected using monoclonal anti-Myc IgG antibody (Oncogene Research Products) at 2 μg/ml, followed by goat anti-mouse IgG (Jackson ImmunoResearch Laboratories) at 1:500 dilution, then streptavidin-conjugated peroxidase (Jackson ImmunoResearch Laboratories) at 1:1000. Peroxidase activity was used to produce a brown precipitate in the presence of Fast DAB (Sigma).

Embryos for sectioning were embedded in 1.5% agar/5% sucrose and frozen in 2-methyl-butane chilled by liquid nitrogen. Sections (10 μm) were obtained using a cryostat microtome.

Whole-mount embryos were cleared in methanol, mounted in 75% glycerol and photographed with a Spot digital camera (Diagnostic Instruments) mounted on a compound microscope. Images of sectioned material were also obtained with the Spot camera.

Antisense morpholino oligonucleotide, DNA and RNA injections

Morpholino antisense oligonucleotides (Gene Tools, LLC.) for *dla* (5′-CTTCTCTTTTCGCCGACTGATTCAT-3′) and *dlc* (5′-AGCACG-TAATAAAACACGAGCCAT-3′) were resuspended in water. Working dilutions of 2.5-5.0 mg/ml were made using 1×Danieau solution and approximately 5 nl injected into one- to two-cell stage embryos collected from matings of wild-type or aei^{AR33}/+ fish using a pressure injector (Applied Scientific Instruments, Inc.). Injected embryos were fixed at yolk-plug closure, three-somite stage or 24 hpf in 4% paraformaldehyde, and were processed for in situ RNA hybridization. Synthetic mRNA encoding the intracellular domain of *Xenopus laevis* Notch1 fused to the Myc tag (NICDMT) (Wettstein et al., 1997) was produced from a construct kindly provided by Chris Kintner using the mMessage Machine kit from Ambion. Approximately 5 nl mRNA at 100 ng/μl was injected into a single cell of eight-cell stage embryos. To make a construct for heat-shock induction of NICDMT, we moved coding sequence from our mRNA expression plasmid and fused it to the zebrafish heat shock 70 promoter (Shoji et al., 1998) in pBluescript and injected approximately 5 nl of the resulting plasmid at 50 μg/μl in the blastodisc of one-cell zygotes. Injected embryos were raised at 28.5°C until shield stage, and subjected to three cycles of 37°C for 15 minutes followed by 28.5°C for 45 minutes. After the end of heat shock cycles, the embryos were raised at 28.5°C until yolk plug closure stage and fixed in 4% paraformaldehyde.

RESULTS

Hypochord cells originate at the lateral border of the midline precursor domain

Previous fate maps revealed that zebrafish floor-plate and notochord precursors arise from the embryonic shield, which is centered on the dorsal margin of gastrula stage embryos (Shih and Fraser, 1995; Melby et al., 1996). However, trunk hypochord precursors have not been placed on any fate map. To identify the location of hypochord precursors, we labeled cells near the margin of shield-stage embryos by photoactivating caged fluorescein. Single labeled cells near the dorsal midline margin produced notochord, whereas clusters of labeled cells centered a few cell diameters farther from the dorsal midline margin gave rise to notochord, floor-plate and ventral neural tube cells, and, occasionally, tail hypochord (data not shown). These observations are consistent with published fate maps (Shih and Fraser, 1995; Melby et al., 1996). We labeled trunk hypochord cells only when we photoactivated clusters of approximately three to five cells at the margin about 15 cell diameters away from the dorsal midline, at the edge of the shield (Fig. 1A,B). Labeled cell clusters that produced only hypochord cells were rare. Instead, we usually observed the following cell types produced by single labeled clusters: hypochord and notochord, hypochord and muscle, hypochord, notochord and muscle, notochord and muscle, or only notochord or muscle (Table 1). We sectioned some 24 hour post fertilization (hpf) embryos that contained labeled hypochord and muscle cells and found that labeled muscle cells were always at the lateral edge of the somite (Fig. 1C), in the position of slow muscle cells (Devoto et al., 1996). We confirmed that these cells were slow muscle by labeling with F59 antibody (Fig. 1D), which identifies zebrafish slow muscle (Devoto et al., 1996). Slow muscle cells arise from adaxial cells, which are next to notochord during gastrulation and early segmentation stages (Devoto et al., 1996). We conclude that hypochord precursors are closely associated with notochord and slow muscle precursors and not with floor-plate precursors in shield stage embryos.

We have begun to follow the movements of labeled

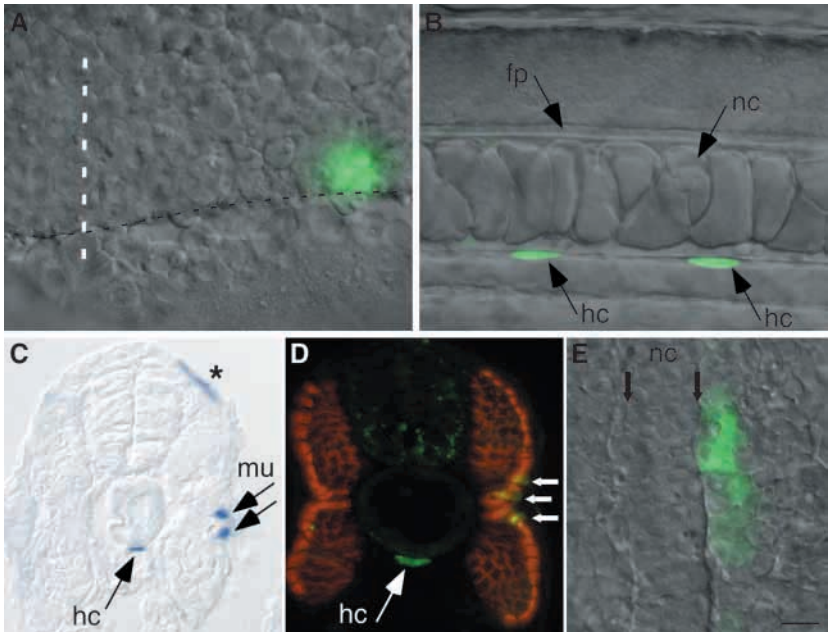

Fig. 1. Hypochord precursors are closely associated with notochord and muscle precursors near the edge of the shield. (A) View of dorsal margin region of 6 hpf (shield stage) embryo. Caged fluorescein was photoactivated in a cluster of three to five cells near the margin (broken black line) and centered about 15 cell diameters from the dorsal midline (broken white line). (B) Side view of trunk region of living embryo at 24 hpf showing labeled hypochord (hc) and notochord (nc) cells. Floor-plate (fp) cells were not labeled. (C) Transverse section of 24 hpf embryo in which the photoactivated fluorescein signal was converted to a blue precipitate. Hypochord, muscle (mu) cells near the periphery of the myotome and periderm (asterisk) were labeled. The periderm precursors were enveloping layer cells that were above the hypochord and muscle precursors at the time of photoactivation. (D) Transverse section of 30 hpf embryo labeled with F59 antibody to reveal slow muscle cells (red). Hypochord (green) and three slow muscle cells (yellow, arrows) were labeled by photoactivated fluorescein. (E) Dorsal view, anterior towards the top, of 9.5 hpf living embryo. Cells labeled by photoactivated fluorescein (green) are next to notochord cells (between arrows). Scale bar: 20 μm for all panels.

hypochord precursors during gastrulation from their starting positions at the edge of the shield to their final positions directly beneath the notochord. Within 1 hour of photoactivation, the cells of the polyclones began to be distributed in the anterior-posterior axis (data not shown). By 3 hours after photoactivation, near the end of the gastrula stage, the labeled cells formed a row next to notochord, which could be identified by morphology (Fig. 1E). Sometimes notochord cells were also labeled. Labeled hypochord cells moved below notochord by about 11-11.5 hpf (data not shown). We conclude from our fate-mapping observations that hypochord precursors originate between notochord precursors and adaxial cells, and migrate to their final positions below the notochord.

Presumptive hypochord precursors express *notch5* and *her4*

Cells bordering the posterior dorsal midline of mid and late gastrula stage embryos express *notch5* and *her4* (Westin and Lardelli, 1997; Takke et al., 1999) (Fig. 2A-D). The distribution of these cells is similar to the distribution of hypochord precursors as they move towards the dorsal midline (see above). To investigate the identity of cells that express *notch5* and *her4*, we examined sectioned material from embryos hybridized with RNA probes. Sagittal and transverse sections of 9.5 hpf embryos at the end of the gastrula stage showed that deep mesendodermal cells, close to the yolk, express *notch5* and *her4* (Fig. 2E-G,I-L). *her4*- or *notch5*-positive cells are next to adaxial cells, marked by *myod* expression (Fig. 2F,G). We never observed cells that express both *notch5* and *myod* or *her4* and *myod*. Cells that express *her4* and *notch5* also were closely associated with *ntl*-positive midline precursors (Fig. 2H-K). Posteriorly, all *her4*-positive cells express *ntl* (Fig. 2I). More anteriorly some *her4*-positive cells express *ntl* but others do not (Fig. 2J). Similarly, some *notch5*-positive cells express *ntl*, whereas others do not (Fig. 2K). The similarity of *her4* and *notch5* RNA distribution indicated that the same cells might express these genes, which we confirmed by double labeling (Fig. 2L).

One interpretation of our data is that some *ntl*-expressing cells at the lateral edges of the midline precursor domain initiate *notch5* and *her4* transcription and that, later, these same cells downregulate *ntl*. Based on our fate map data described above, we predict that these cells are hypochord precursors. Consistent with this prospect, after gastrula stage, by 11.5 hpf, *notch5*- and *her4*-expressing cells occupy a single row ventral to notochord, where hypochord cells differentiate (Fig. 2M and data not shown).

The coincident expression of *notch5* and *her4* is consistent with the possibility that Notch5 activity promotes *her4* expression. However, we detect *her4* RNA at the same time or, perhaps, slightly earlier than *notch5* RNA. Midline cells express at least two other *notch* genes, *notch1a* and *notch1b* (Bierkamp and Campos-Ortega, 1993; Westin and Lardelli, 1997) (Fig. 2N). This observation opens the possibility that

Table 1. Fates of cells labeled as clusters at the edge of the embryonic shield

Hypochord only	Hypochord and notochord	Hypochord and muscle	Hypochord and notochord and muscle	Notochord and muscle	Notochord only	Muscle only	Total embryos
6%	9%	16%	14%	6%	33%	17%	70

Caged fluorescein was photoactivated in clusters containing three to five cells located at the embryonic margin of shield-stage embryos, ~15 cell diameters from the dorsal midline. Embryos were analyzed at 24 hpf for presence of labeled hypochord, floor-plate, notochord and muscle cells. No labeled floor-plate cells appeared in these polyclones. Percentages indicate fraction of polyclone labels that produced the cell types in each category.

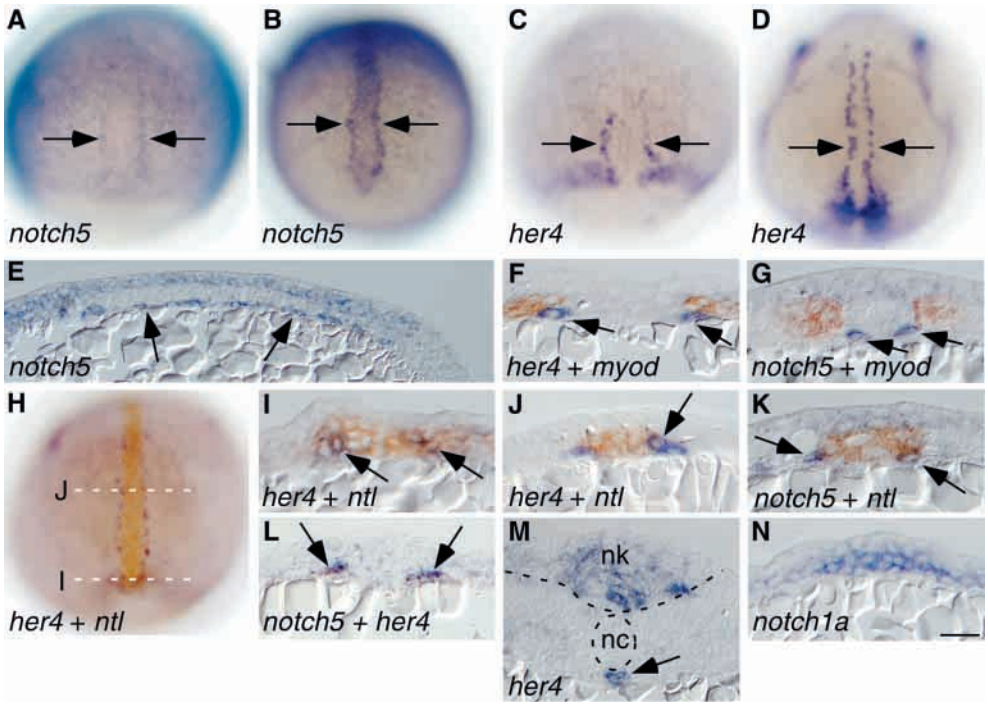

Fig. 2. Presumptive hypochord precursors express *notch5* and *her4*. (A,B) Dorsal views, anterior towards the top, of 8.5 hpf (A) and 9.5 hpf (B) embryos probed for *notch5* expression. Cells near the dorsal midline express *notch5* (arrows). (C,D) Dorsal views, anterior towards the top, of 8.5 hpf (C) and 9.5 hpf (D) embryos probed for *her4* expression. Cells near the dorsal midline express *her4* (arrows). (E) Sagittal section, anterior towards the left, of 9.5 hpf embryo probed for *notch5* expression. Deep mesendodermal cells express *notch5* (arrows). (F) Transverse section of 9.5 hfp embryo probed for *her4* (blue, arrows) and *myod* (red) expression. Adaxial cells, marked by *myod* expression, do not express *her4*. (G) Transverse section of 10 hpf embryo probed for *notch5* (blue, arrows) and *myod* (red) expression. *myod*-positive adaxial cells do not express *notch5*. (H) Dorsal view, anterior towards the top, of 9.5 hpf embryo probed for *her4* (blue) and *ntl* (red) expression. Broken lines indicate approximate positions of transverse sections shown in I,J. (I,J) Transverse sections of 9.5 hpf embryo probed for *her4* (blue) and *ntl* (red) expression. (I) Posterior transverse section with several double-labeled cells (arrows). (J) Anterior transverse section in which one *her4*-positive cell expresses *ntl* (arrow) whereas two others do not. (K) Transverse section of 9.5 hpf embryo probed for *notch5* (blue, arrows) and *ntl* (red) expression. The *notch5*-positive cell on the right expresses *ntl* whereas the one on the left does not. (L) Transverse section of 9.5 hpf embryo probed for *notch5* (blue) and *her4* expression. Cells bordering the midline express both genes (arrows). (M) Transverse section of 11.5 hpf embryo probed for *her4* expression. A single hypochord cell (arrow), ventral to notochord (nc), and neural keel (nk) cells expresses *her4*. (N) Transverse section of YPC stage embryo probed for *notch1a* expression. Many dorsal mesoderm cells express *notch1a*. Scale bar: 100 μm for A-D,H; 50 μm for E; 25 μm for I-N.

multiple Notch receptors promote *her4* transcription in presumptive hypochord precursors.

Taken together, our data indicate that hypochord precursors arise at the lateral edges of the *ntl*-expressing midline precursor domain and that similarly positioned *notch5/her4*-positive presumptive hypochord precursors downregulate *ntl* expression. These observations raise the possibility that hypochord cells originate as *ntl*-expressing midline precursors.

deltaD and *deltaC*-expressing cells border presumptive hypochord precursors

Gastrulation stage zebrafish embryos express three of four known Delta genes. During mid and late gastrulation stages, embryos express *dla* uniformly, except for a few cells near the dorsal midline margin that transiently express *dla* at elevated levels (Appel et al., 1999). By contrast, paraxial mesoderm, but not axial mesoderm, strongly expresses *dlc* and *dld* (Dornseifer et al., 1997; Haddon et al., 1998) (Fig. 3A-F). Double labeling experiments showed that *dlc* and *dld*-expressing cells are adjacent to *ntl*-positive midline precursors (Fig. 3G,H and data not shown). Additionally, we found that *dlc*-positive cells are next to *her4*-expressing cells (Fig. 3I). This raises the possibility that *her4* expression is induced by DeltaC and DeltaD ligands expressed by neighboring paraxial mesoderm cells.

Hypochord specification requires *delta* functions

We used loss-of-function strategies to test the role of Delta-Notch signaling in hypochord specification. Previously, we showed that dla^{dx2} mutant embryos, with incomplete penetrance and variable expressivity, had fewer hypochord cells than wild-type embryos (Appel et al., 1999). Likewise, aei^{AR33} mutant embryos, which lack *dld* function (Holley et al., 2000), have an incompletely penetrant and variable reduction of hypochord cell number (Fig. 4B; Table 2). We do not know of a *dlc* mutation, thus, we injected wild-type embryos with *dlc* antisense morpholino oligonucleotides (MO) to interfere with *dlc* translation (Heasman et al., 2000; Nasevicius and Ekker, 2000). On average, injected embryos also had fewer hypochord cells than uninjected embryos (Fig. 4C; Table 2). These data raise the possibility that Delta genes are functionally redundant for hypochord development. To test this, we injected embryos produced by intercrosses of heterozygous aei^{AR33} adults with approximately 25 ng *dlc* MO, a dose that did not produce morphological defects when injected into wild-type embryos (data not shown). At 24 hpf, injected homozygous aei^{AR33} mutant embryos were identified by the somite defect that results from loss of *dld* function (van Eeden et al., 1996; Holley et al., 2000). Very few hypochord cells developed in homozygous aei^{AR33} mutant embryos injected with *dlc* MO (Fig. 4D; Table 2). This result supports the idea that *dlc* and *dld* have redundant functions in hypochord development. Within the sibling embryos, we could identify two classes; approximately one-third had hypochord defects similar to wild-type embryos injected with *dlc* MO, whereas approximately two-thirds had hypochord phenotypes

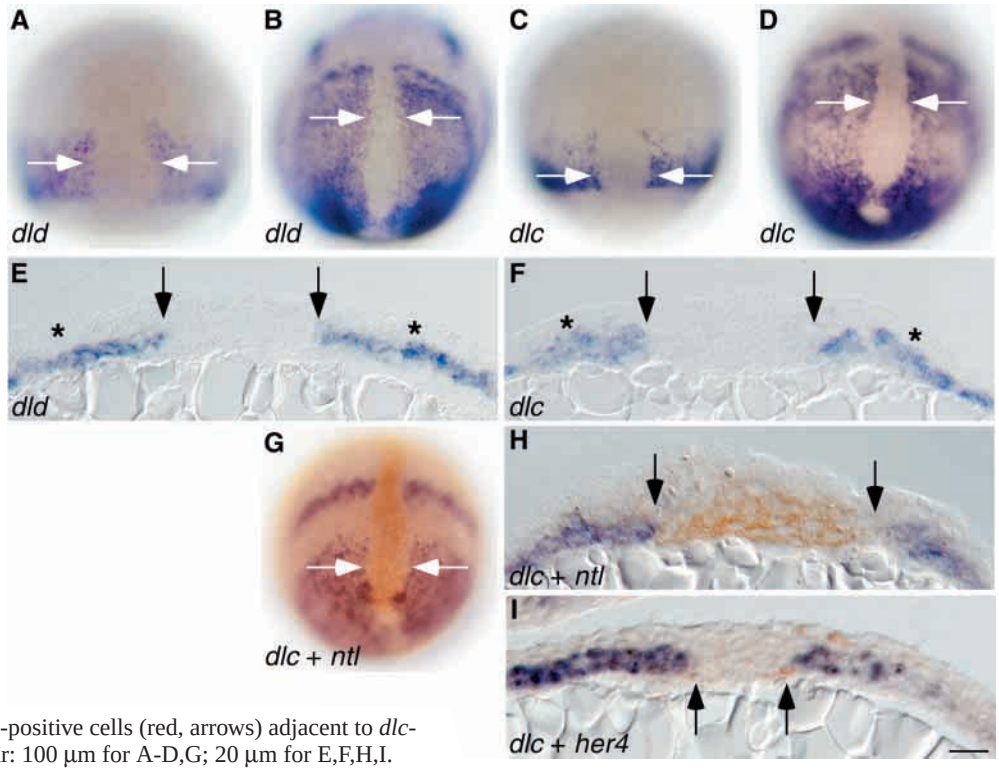

Fig. 3. Paraxial mesoderm cells next to midline precursors express *dlc* and *dld*. (A,B) Dorsal views, anterior towards the top, of 8.5 hpf (A) and 9.5 hpf (B) embryos probed for *dld* expression. Cells at the dorsal midline (arrows) do not express *dld*. (C,D) Dorsal views, anterior towards the top, of 8.5 hpf (C) and 9.5 hpf (D) embryos probed for *dlc* expression. Similar to *dld*, dorsal midline cells (arrows) do not express *dlc*. (E,F) Transverse sections of 9.5 hpf embryos probed for *dld* (E) and *dlc* (F) expression. Paraxial mesoderm expresses *dld* and *dlc*, whereas midline (flanked by arrows) and ectoderm (asterisks) do not. (G) Dorsal view, anterior towards the top, of 9.5 hpf embryo probed for *dlc* (purple) and *ntl* (red) expression. (H) Transverse section of 9.5 hpf embryo probed for *dlc* (blue) and *ntl* (red) expression. In both G and H, *dlc*-expressing paraxial mesoderm borders *ntl*-positive midline precursors (arrows). (I) Transverse section of 9.5 hpf embryo showing *her4*-positive cells (red, arrows) adjacent to *dlc*-expressing cells (blue, arrows). Scale bar: 100 μm for A-D,G; 20 μm for E,F,H,I.

intermediate to wild-type and homozygous *aei*^{AR33} mutant embryos injected with *dlc* MO (data not shown). We speculate that these two classes represent homozygous wild-type and heterozygous *aei*^{AR33} mutant embryos, respectively. We also tested loss of *dla* function by MO injection. We observed only small gaps in the hypochords of some of the wild-type embryos injected with *dla* MO (Table 2). However, *aei*^{AR33} mutant embryos injected with *dla* MO had fewer hypochord cells than uninjected *aei*^{AR33} mutant embryos (Table 2). Therefore, *dla* function also may contribute to hypochord development. These data support the possibility that paraxial mesoderm expression of *dld* and *dlc* and uniform expression of *dla* promote hypochord development.

We have identified *her4*-expressing cells as hypochord precursors and Notch activity regulates *her4* expression (Takke et al., 1999). To test if *her4* expression by presumptive hypochord precursors requires Delta functions, we injected embryos produced by heterozygous *aei*^{AR33} adults with *dlc* MO and examined them at 9.5 hpf. Of 49 embryos probed for *her4*, 17 (35%) had substantially fewer *her4*-expressing cells (Fig. 4F) and 11 (22%) had no *her4*-expressing cells (Fig. 4G). These data indicate that DeltaC and DeltaD ligands promote *her4* expression. By contrast, all injected embryos expressed *notch5* normally (Fig. 4E) indicating that *notch5* expression by presumptive hypochord precursors does not require DeltaC and DeltaD. Taken together with our expression pattern data, these observations provide strong evidence that DeltaC and DeltaD, expressed by adaxial cells, induce *her4* expression in neighboring midline precursors during gastrulation, specifying them for hypochord fate.

To test the specificity of our MO effects we examined primary neurogenesis. Neural plate cells express *dla* and *dld* but not *dlc* (Dornseifer et al., 1997; Appel and Eisen, 1998; Haddon et al., 1998). *dla*^{dx2} mutant embryos have a large excess of primary neurons, perhaps because of the dominant negative nature of the allele (Appel et al., 1999; Appel et al., 2001). *aei*^{AR33} mutant embryos have only a small increase in the number of primary neurons (Holley et al., 2000) (Fig. 4I). Twenty-four percent of embryos (22/90 embryos) produced by an intercross of *aei*^{AR33}/+ adults and injected with approximately 25 ng *dlc* MO had primary neuron phenotypes similar to uninjected *aei*^{AR33} homozygous mutant embryos (Fig. 4J). Thus, reduction of *dlc* function did not appear to enhance the neural phenotype produced by loss of *dld* function, indicating that the *dlc* MO did not interfere, nonspecifically, with neurogenesis. By contrast, we found that injection of *dla* MO produced excess primary neurons in a dose-dependent manner when injected into wild-type embryos (data not shown). Injection of approximately 5 ng *dla* MO, which did

Table 2. Effect of loss of Delta functions on hypochord development

Genotype and antisense morpholino	% Embryos with reduced hypochord	Average number of hypochord cells
Wild type	0% (*n*=10)	43
aei^{-}/*aei*$^{-}$	36% (*n*=11)	28 (*P*<0.001)
wt; *dlc* MO	69% (*n*=39)	27 (*P*<0.001)
aei^{-}/*aei*$^{-}$; *dlc* MO	100% (*n*=19)	3 (*P*<0.001)
wt; *dla* MO	6% (*n*=52)	37 (*P*<0.06)
aei^{-}/*aei*$^{-}$; *dla* MO	91% (*n*=11)	11 (*P*<0.001)

Embryos were injected with approximately 25 ng *dlc* or 5 ng *dla* antisense morpholino oligonucleotide (MO). Hypochord was analyzed in 24-26 hpf embryos hybridized with *col2a1* probe. *n*, the total number of embryos analyzed for each experiment. Hypochord cells were counted between somites 1 and 17. *P* values are based on analysis of 9-11 embryos, compared with wild type, for each experiment.

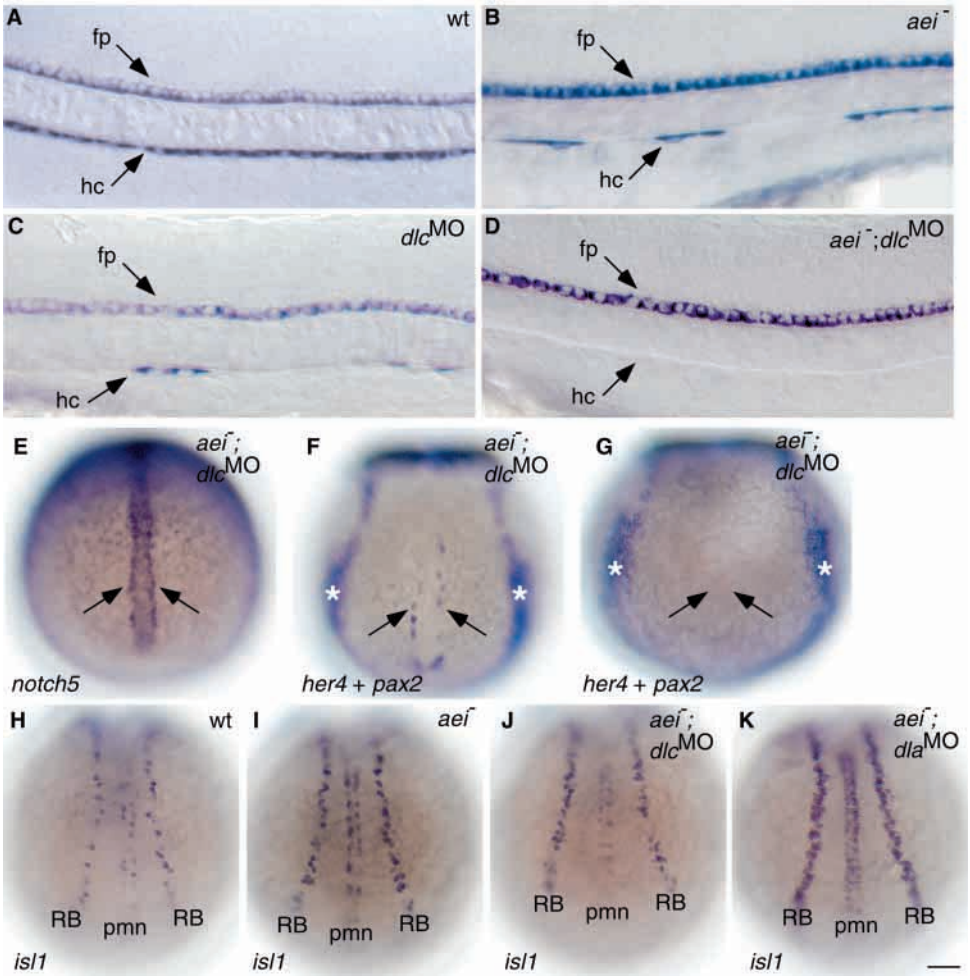

Fig. 4. Delta functions are required for hypochord development. (A-F) Side views, anterior towards the left, of the trunk region of 24-26 hpf embryos probed for *col2a1* expression to mark floor-plate (fp) and hypochord (hc) cells. (A) Wild-type embryo showing the normal pattern of floor-plate and hypochord cells. (B) Homozygous mutant *aei*^{AR33} embryo with a deficit of hypochord cells. Floor plate appeared normal. (C) Wild-type embryo injected with *dlc* antisense morpholino oligonucleotides (MO). Hypochord cell number was reduced, whereas floor plate appeared normal. (D) Homozygous mutant *aei*^{AR33} embryo injected with *dlc* MO. Most hypochord cells were absent, whereas floor plate appeared normal. (E-G) Dorsal views, anterior towards the top, of 9.5 hpf embryos from *aei*^{AR33}/+ intercross injected with *dlc* MO. *notch5* expression was normal (E), whereas *her4* expression was reduced (F) or absent (G) (compare with Fig. 2D). Embryos in F,G were double-labeled to reveal *pax2.1* expression in pronephros (asterisks), which was normal. (H-K) Dorsal views, anterior towards the top, of 10.5 hpf embryos probed for *isl1* expression to reveal prospective Rohon-Beard (RB) neurons and primary motoneurons (pmn). (H) Wild-type, uninjected embryo. (I) *aei*^{AR33} mutant embryo showing small increase in the number of prospective primary motoneurons and RBs. (J) Embryo from *aei*^{AR33}/+ intercross injected with *dlc* MO. The neural phenotype is similar to that of the uninjected *aei*^{AR33} mutant embryo shown in I. (K) Embryo from *aei*^{AR33}/+ intercross injected with *dla* MO. The number of prospective primary motoneurons and RB cells was greater than the embryos shown in I,J. Scale bar: 20 μm in A-D; 80 μm in E-K.

not cause a strong neural phenotype in wild-type embryos, greatly enhanced the neural phenotype of *aei*^{AR33} mutant embryos (17/74 embryos; 23%) (Fig. 4K). As the *dla* and *dlc* MO phenotypes correlate with the *dla* and *dlc* expression patterns, we conclude that the MO effects are specific to their intended targets.

Notch signaling represses ntl expression by midline precursors

One interpretation of our results is that Delta signaling, primarily from paraxial mesoderm, to midline precursors expressing Notch receptors inhibits *ntl* expression and promotes *her4* expression, consequently instructing these cells to develop as hypochord. We tested this by expressing a constitutively active form of Notch. To perform these experiments, we found it necessary to limit the number of cells that expressed constitutively active Notch so that embryos would develop fairly normally. First, we confirmed and extended a previous observation that Notch activity promotes *her4* expression (Takke et al., 1999) by using a heat shock promoter (Shoji et al., 1998) to express during gastrulation a constitutively active form of *X. laevis Notch1* (Wettstein et al., 1997) fused to the Myc tag (NICDMT). This resulted in embryos that had ligand-independent Notch activity in some but not all cells. Of 57 injected embryos, 44 had numerous cells that expressed NICDMT, identified by staining for the fused Myc epitope. Many of these cells expressed *her4* (data not shown). Analysis of sectioned embryos revealed that NICDMT-positive cells ectopically expressed *her4* (Fig. 5A). We never saw ectopic *her4*-expressing cells that did not express NICDMT, indicating that Notch induction of *her4* expression is cell autonomous. Next, we injected one cell of eight-cell stage embryos with synthetic mRNA encoding NICDMT, raised the embryos to the end of the gastrula stage and probed for *ntl* expression. Twenty-two of 116 (19%) injected embryos had midline cells that expressed NICDMT; the *ntl* expression domain was reduced in each of these indicating that unregulated Notch activity in midline precursor cells inhibits *ntl* expression (Fig. 5B,C). Tissue sections revealed that NICDMT-positive midline cells did not express *ntl*, whereas neighboring cells did (Fig. 5D), indicating that Notch activity cell autonomously inhibits *ntl* expression. Together, these observations show that Notch activity can inhibit *ntl* expression and promote *her4* expression, consistent with our hypothesis

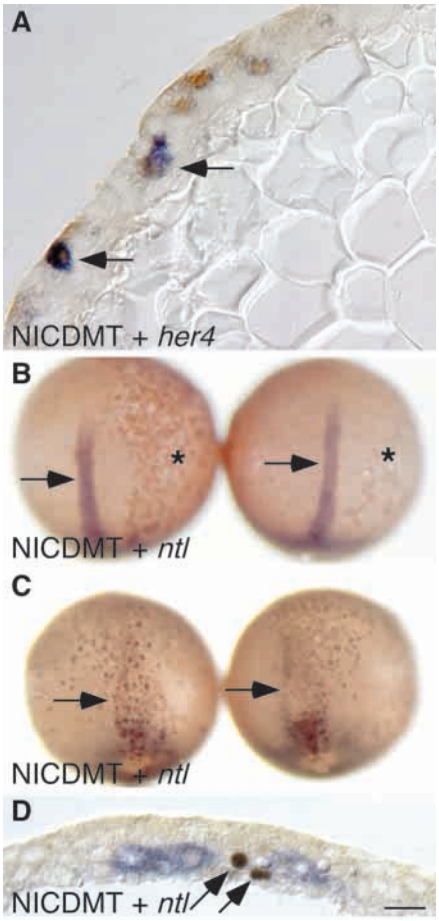

Fig. 5. Constitutive Notch activity promotes *her4* and inhibits *ntl* expression. (A) Transverse section showing lateral region of 9.5 hpf embryo in which NICDMT expression was induced during gastrulation. Some cells that expressed NICDMT (brown) also expressed *her4* (blue, arrows). (B,C) Dorsal views, anterior towards the top, of 9.5 hpf embryos labeled for *ntl* (blue) and NICDMT (brown) expression. These embryos were injected with mRNA encoding NICDMT in a single cell at the eight-cell stage. (B) Embryos in which NICDMT-positive cells were restricted to ventrolateral regions (asterisks). Midline cells expressed *ntl* normally (arrows). (C) Embryos in which NICDMT-expressing cells occupied the dorsal midline region. These embryos had fewer midline cells that expressed *ntl* (arrows). (D) Transverse section through dorsal midline region of 9.5 hpf embryo treated as embryos described in B,C. Two NICDMT-positive cells (brown, arrows) occupied the notochord precursor domain but did not express *ntl* (blue), whereas neighboring cells expressed *ntl* normally. Scale bar: 20 μm in A,D; 120 μm in B,C.

that Delta-Notch signaling induces a subset of midline precursors to develop as hypochord.

DISCUSSION

We have shown previously that *dla* mutant embryos have excess notochord cells and deficits of floor-plate and hypochord cells, whereas wild-type embryos injected with *dla* mRNA have fewer notochord cells and excess floor-plate and hypochord cells (Appel et al., 1999). We hypothesized that

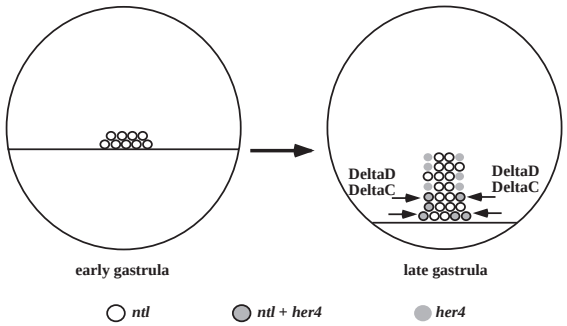

Fig. 6. Model for Delta-Notch-mediated induction of hypochord fate. At early gastrula stage, *ntl*-expressing midline precursors occupy the dorsal margin. During gastrulation, Delta signaling, primarily from paraxial mesoderm expression of DeltaD and DeltaC, induce *ntl*-positive midline precursors to express *her4*. These cells downregulate *ntl* expression and, after completion of gastrulation, migrate beneath notochord to form hypochord.

Delta-Notch signaling during gastrulation mediated cell fate decisions made by midline precursors. However, because we did not know the exact spatial relationships of midline precursors, we could not determine the mechanisms by which Delta-Notch signaling mediated midline cell specification. We have considered two broad possibilities. First, midline precursors might have equivalent developmental potential. Delta-Notch signaling between neighboring cells might, in a process called lateral specification (Artavanis-Tsakonas et al., 1995; Greenwald, 1998), cause midline precursors to take different fates. An example of this type of mechanism is specification of the anchor cell and ventral uterine precursor cell during formation of the *Caenorhabditis elegans* gonad (Seydoux and Greenwald, 1989). In this case, we would expect zebrafish midline precursors to be intermixed. Second, midline precursors might be induced to develop differently by Delta-Notch-mediated signals from a separate cell population, similar to the way that equivalent blastomeres are specified for different fates by signaling from a nonequivalent blastomere in *C. elegans* (Mickey et al., 1996). We would predict that midline precursors that produce different cell types occupy distinct positions relative to the source of inductive signal. Our results from a combination of fate mapping, gene expression pattern analyses and tests of gene function lead us to favor the latter mechanism for specification of hypochord cells in zebrafish. Specifically, we propose that, during gastrulation, high levels of Delta signals from paraxial mesoderm induce neighboring midline precursors to develop as hypochord cells, whereas nearby midline precursors not exposed to high levels of Delta signals develop as notochord (Fig. 6).

Zebrafish hypochord precursors arise from the lateral edge of the shield

Our data indicate that hypochord precursors are not intermixed with other precursors throughout the shield but occupy a distinct domain at the lateral edges of the shield. When we labeled small clusters of cells at the lateral edge of the shield, those that gave rise to hypochord often also produced notochord and/or slow muscle. Rarely, if ever, did these polyclones also comprise floor-plate and other ventral neural cells, fast muscle cells or endoderm. By contrast we never

observed trunk hypochord cells in polyclones that originated at the dorsal midline, although we occasionally did see tail hypochord cells. Thus, trunk hypochord precursors apparently arise only from the lateral edges of the shield, in close association with notochord and slow muscle precursors. Because of the small number of hypochord precursors, we currently are unable to determine the precise arrangement of hypochord, notochord and slow muscle precursors. However, our data showing that hypochord precursors map to the edge of the shield, coincident with the edge of the notochord precursor domain (Shih and Fraser, 1995; Melby et al., 1996), are consistent with our hypothesis that hypochord cells are specified from midline precursors by an inductive signal from muscle precursors.

Fate mapping of axolotl and histological analyses of frog and fish embryos indicated that hypochord is derived from endoderm (Lofberg and Collazo, 1997; Cleaver et al., 2000; Eriksson and Lofberg, 2000). However, labeled hypochord cells did not appear in a fate map of zebrafish endoderm (Warga and Nusslein-Volhard, 1999). In addition, mutations of *one-eyed-pinhead* and *casanova*, which are required for endoderm development (Schier et al., 1997; Alexander et al., 1999), do not result in loss of trunk hypochord (Alexander et al., 1999) (and data not shown). Our data showing hypochord precursors are closely associated with precursors of other mesodermal cell types at the onset of gastrulation indicate that zebrafish hypochord originates from mesoderm and not endoderm.

Distinct cell populations express Delta and Notch genes

Previous publications showed that cells that form two columns on either side of the midline of late-gastrulation stage embryos transcribe *notch5* and *her4* (Westin and Lardelli, 1997; Takke et al., 1999). We demonstrated here that the same cells expressed *notch5* and *her4*, and that they were deep within the mesoderm, close to the yolk. The distribution of *notch5*- and *her4*-expressing cells during late gastrula stage was similar to distribution of photoactivated cells that went on to produce hypochord. After gastrula stage, *notch5*- and *her4*-expressing cells were ventral to notochord, in the final position of hypochord. We also found that cells that expressed *notch5* and *her4* during late gastrulation were next to adaxial cells, the slow muscle precursors. This is consistent with our fate-mapping results that hypochord-containing polyclones often contained slow muscle cells. *notch5*- and *her4*-expressing cells also were close to *ntl*-positive midline precursors, again consistent with our observations that polyclones often contained both hypochord and notochord cells. Thus, *notch5*- and *her4*-expressing cells are probably hypochord precursors.

We showed previously that gastrulating embryos express *dla* uniformly, except for transient upregulation at the dorsal midline (Appel et al., 1999). Thus, the pattern of *dla* transcription does not predict the pattern of hypochord precursor specification. We now show that paraxial mesoderm, which includes adaxial cells adjacent to midline precursors, expresses *dlc* and *dld*. Thus, adaxial cells could be the primary source of Delta signals that induce hypochord development.

Delta function is required for hypochord specification

Results from our loss-of-function experiments support the idea that *dlc* and *dld* signaling from adaxial cells induce hypochord development and also indicate that *dla* may contribute to hypochord specification. Embryos that lack *dld* function, by mutation, or have reduced *dlc* function, by MO injection, have incompletely penetrant and variably expressive hypochord phenotypes. By contrast, all embryos that lack both *dlc* and *dlc* functions have very few hypochord cells, indicating that *dld* and *dlc* are functionally redundant for hypochord specification. We showed previously that embryos having the dominant negative dla^{dx2} mutant allele have fewer hypochord cells (Appel et al., 1999). This mutant allele, which is predicted to substitute tyrosine for a conserved cysteine in the second EGF repeat of the extracellular domain, may produce DeltaA protein that can interfere with the functions of DeltaD and DeltaC, perhaps by forming heterodimers. As gastrulating embryos uniformly express *dla* transcripts, mutant DeltaA protein could interfere with the hypochord-inducing functions of DeltaD and DeltaC. However, we found here that reduction of *dla* function by antisense morpholino oligonucleotide injection also reduced the number of hypochord cells in wild-type embryos and enhanced the penetrance and expressivity of the *aei/dld* mutant phenotype. This apparent requirement for *dla* activity raises the question of whether a localized source of Notch ligand can fully account for the pattern of hypochord specification. However, *dla* is not sufficient to specify hypochord in the absence of *dlc* and *dld*. Thus, we propose that high levels of Delta proteins produced by adaxial cells are required to induce midline precursors to develop as hypochord (Fig. 6).

How might Delta signals induce hypochord development? One key might be regulation of *ntl* expression. *ntl* mutant embryos lack notochord and rostral hypochord and have excess floor plate (Rissi et al., 1995; Halpern et al., 1997). Halpern et al. (Halpern et al., 1997) proposed that *ntl* regulates a midline precursor fate decision by promoting notochord and inhibiting floor-plate development. We propose that modulation of *ntl* expression within midline precursors by Delta-Notch signaling is required for hypochord development. In our model, *ntl* promotes formation of a population of midline precursors that have the potential to develop either as notochord or hypochord. Activation of Notch in a subset of precursors by Delta ligands expressed by neighboring paraxial mesoderm cells induces *her4* and represses *ntl* expression. Consistent with this, we show here that constitutive Notch activity can cell-autonomously drive ectopic *her4* expression. In the absence of Notch activity, *her4* expression is not induced, as we demonstrated here, and excess midline cells express *ntl*, as we showed previously (Appel et al., 1999). Thus, Notch activity diverts midline precursors from notochord to hypochord fate.

As *her4* is a member of the *hairy-Enhancer of split* gene family, which generally encode transcription repressors (reviewed by Fisher and Caudy, 1998), Notch inhibition of *ntl* expression could occur via direct action of Her4 on *ntl* regulatory elements. Notably, in the tunicate *Ciona intestinalis*, Notch activity promotes expression of the *Brachyury* gene, apparently by direct binding of Supressor of Hairless (Corbo et al., 1997; Corbo et al., 1998). Direct comparison of the regulatory DNA that controls expression of *Brachyury* homologs in tunicates and zebrafish may provide interesting insights to the evolution of the embryonic midline.

Thanks to Lila Solnica-Krezel and Jacek Topczewski for comments on the manuscript, to Marnie Halpern for discussions, to Frank Stockdale, John Kuwada, Michael Lardelli, José Campos-Ortega and Chris Kintner for reagents, and to the Vanderbilt zebrafish facility staff for fish care. This work was supported by NIH grant HD38118.

REFERENCES

Alexander, J., Rothenberg, M., Henry, G. L. and Stainier, D. Y. (1999). casanova plays an early and essential role in endoderm formation in zebrafish. *Dev. Biol.* **215**, 343-357.

Appel, B., Korzh, V., Glasgow, E., Thor, S., Edlund, T., Dawid, I. B. and Eisen, J. S. (1995). Motoneuron fate specification revealed by patterned LIM homeobox gene expression in embryonic zebrafish. *Development* **121**, 4117-4125.

Appel, B. and Eisen, J. S. (1998). Regulation of neuronal specification in the zebrafish spinal cord by Delta function. *Development* **125**, 371-380.

Appel, B., Fritz, A., Westerfield, M., Grunwald, D. J., Eisen, J. S. and Riley, B. B. (1999). Delta-mediated specification of midline cell fates in zebrafish embryos. *Curr. Biol.* **9**, 247-256.

Appel, B., Givan, L. A. and Eisen, J. S. (2001). Delta-Notch signaling and lateral inhibition in zebrafish spinal cord development. *BMC Dev. Biol.* **1**, 13.

Artavanis-Tsakonas, S., Matsuno, K. and Fortini, M. E. (1995). Notch signaling. *Science* **268**, 225-232.

Bierkamp, C. and Campos-Ortega, J. A. (1993). A zebrafish homologue of the Drosophila neurogenic gene Notch and its pattern of transcription during early embryogenesis. *Mech. Dev.* **43**, 87-100.

Catala, M., Teillet, M. A., de Robertis, E. M. and le Douarin, M. L. (1996). A spinal cord fate map in the avian embryo: while regressing, Hensen's node lays down the notochord and floor plate thus joining the spinal cord lateral walls. *Development* **122**, 2599-2610.

Cleaver, O. and Krieg, P. A. (1998). VEGF mediates angioblast migration during development of the dorsal aorta in Xenopus. *Development* **125**, 3905-3914.

Cleaver, O., Seufert, D. W. and Krieg, P. A. (2000). Endoderm patterning by the notochord: development of the hypochord in Xenopus. *Development* **127**, 869-879.

Corbo, J. C., Levine, M. and Zeller, R. W. (1997). Characterization of a notochord-specific enhancer from the Brachyury promoter region of the ascidian, Ciona intestinalis. *Development* **124**, 589-602.

Corbo, J. C., Fujiwara, S., Levine, M. and di Gregorio, A. (1998). Suppressor of hairless activates brachyury expression in the Ciona embryo. *Dev. Biol.* **203**, 358-368.

Devoto, S. H., Melancon, E., Eisen, J. S. and Westerfield, M. (1996). Identification of separate slow and fast muscle precursor cells in vivo, prior to somite formation. *Development* **122**, 3371-3380.

Dornseifer, P., Takke, C. and Campos-Ortega, J. A. (1997). Overexpression of a zebrafish homologue of the Drosophila neurogenic gene Delta perturbs differentiation of primary neurons and somite development. *Mech. Dev.* **63**, 159-171.

Eriksson, J. and Lofberg, J. (2000). Development of the hypochord and dorsal aorta in the zebrafish embryo (Danio rerio). *J. Morphol.* **244**, 167-176.

Fisher, A. and Caudy, M. (1998). The function of hairy-related bHLH repressor proteins in cell fate decisions. *BioEssays* **20**, 298-306.

Gont, L. K., Steinbeisser, H., Blumberg, B. and de Robertis, E. M. (1993). Tail formation as a continuation of gastrulation: the multiple cell populations of the Xenopus tailbud derive from the late blastopore lip. *Development* **119**, 991-1004.

Greenwald, I. (1998). LIN-12/Notch signaling: lessons from worms and flies. *Genes Dev.* **12**, 1751-1762.

Haddon, C., Smithers, L., Schneider-Maunoury, S., Coche, T., Henrique, D. and Lewis, J. (1998). Multiple delta genes and lateral inhibition in zebrafish primary neurogenesis. *Development* **125**, 359-370.

Halpern, M. E., Hatta, K., Amacher, S. L., Talbot, W. S., Yan, Y. L., Thisse, B., Thisse, C., Postlethwait, J. H. and Kimmel, C. B. (1997). Genetic interactions in zebrafish midline development. *Dev. Biol.* **187**, 154-170.

Hauptmann, G. and Gerster, T. (2000). Multicolor whole-mount in situ hybridization. *Methods Mol. Biol.* **137**, 139-148.

Heasman, J., Kofron, M. and Wylie, C. (2000). Beta-catenin signaling activity dissected in the early Xenopus embryo: a novel antisense approach. *Dev. Biol.* **222**, 124-134.

Holley, S. A., Geisler, R. and Nusslein-Volhard, C. (2000). Control of her1 expression during zebrafish somitogenesis by a delta- dependent oscillator and an independent wave-front activity. *Genes Dev.* **14**, 1678-1690.

Jowett, T. (2001). Double in situ hybridization techniques in zebrafish. *Methods* **23**, 345-358.

Kimmel, C. B., Ballard, W. W., Kimmel, S. R., Ullmann, B. and Schilling, T. F. (1995). Stages of embryonic development of the zebrafish. *Dev. Dyn.* **203**, 253-310.

Lofberg, J. and Collazo, A. (1997). Hypochord, an enigmatic embryonic structure: study of the axolotl embryo. *J. Morphol.* **232**, 57-66.

Melby, A. E., Warga, R. M. and Kimmel, C. B. (1996). Specification of cell fates at the dorsal margin of the zebrafish gastrula. *Development* **122**, 2225-2237.

Mickey, K. M., Mello, C. C., Montgomery, M. K., Fire, A. and Priess, J. R. (1996). An inductive interaction in 4-cell stage C. elegans embryos involves APX-1 expression in the signalling cell. *Development* **122**, 1791-1798.

Nasevicius, A. and Ekker, S. C. (2000). Effective targeted gene 'knockdown' in zebrafish. *Nat. Genet.* **26**, 216-220.

Rissi, M., Wittbrodt, J., Delot, E., Naegeli, M. and Rosa, F. M. (1995). Zebrafish Radar: a new member of the TGF-beta superfamily defines dorsal regions of the neural plate and the embryonic retina. *Mech. Dev.* **49**, 223-234.

Schier, A. F., Neuhauss, S. C., Helde, K. A., Talbot, W. S. and Driever, W. (1997). The one-eyed pinhead gene functions in mesoderm and endoderm formation in zebrafish and interacts with no tail. *Development* **124**, 327-342.

Schoenwolf, G. C. and Sheard, P. (1990). Fate mapping the avian epiblast with focal injections of a fluorescent- histochemical marker: ectodermal derivatives. *J. Exp. Zool.* **255**, 323-339.

Schulte-Merker, S., van Eeden, F. J., Halpern, M. E., Kimmel, C. B. and Nusslein-Volhard, C. (1994). no tail (ntl) is the zebrafish homologue of the mouse T (Brachyury) gene. *Development* **120**, 1009-1015.

Selleck, M. A. and Stern, C. D. (1991). Fate mapping and cell lineage analysis of Hensen's node in the chick embryo. *Development* **112**, 615-626.

Serbedzija, G. N., Chen, J. N. and Fishman, M. C. (1998). Regulation in the heart field of zebrafish. *Development* **125**, 1095-1101.

Seydoux, G. and Greenwald, I. (1989). Cell autonomy of lin-12 function in a cell fate decision in C. elegans. *Cell* **57**, 1237-1245.

Shih, J. and Fraser, S. E. (1995). Distribution of tissue progenitors within the shield region of the zebrafish gastrula. *Development* **121**, 2755-2765.

Shoji, W., Yee, C. S. and Kuwada, J. Y. (1998). Zebrafish semaphorin Z1a collapses specific growth cones and alters their pathway in vivo. *Development* **125**, 1275-1283.

Spemann, H. (1938). *Embryonic Development and Induction*. New York: Yale University Press.

Stickney, H. L., Barresi, M. J. and Devoto, S. H. (2000). Somite development in zebrafish. *Dev. Dyn.* **219**, 287-303.

Takke, C., Dornseifer, P., Weizsacker, E. and Campos-Ortega, J. A. (1999). her4, a zebrafish homologue of the Drosophila neurogenic gene E(spl), is a target of NOTCH signalling. *Development* **126**, 1811-1821.

Tanabe, Y. and Jessell, T. M. (1996). Diversity and pattern in the developing spinal cord. *Science* **274**, 1115-1123.

van Eeden, F. J., Granato, M., Schach, U., Brand, M., Furutani-Seiki, M., Haffter, P., Hammerschmidt, M., Heisenberg, C. P., Jiang, Y. J., Kane, D. A. et al. (1996). Mutations affecting somite formation and patterning in the zebrafish, Danio rerio. *Development* **123**, 153-164.

Warga, R. M. and Nusslein-Volhard, C. (1999). Origin and development of the zebrafish endoderm. *Development* **126**, 827-838.

Weinberg, E. S., Allende, M. L., Kelly, C. S., Abdelhamid, A., Murakami, T., Andermann, P., Doerre, O. G., Grunwald, D. J. and Riggleman, B. (1996). Developmental regulation of zebrafish MyoD in wild-type, no tail and spadetail embryos. *Development* **122**, 271-280.

Westin, J. and Lardelli, M. (1997). Three novel *Notch* genes in zebrafish: implications for vertebrate *Notch* gene evolution and function. *Dev. Genes Evol.* **207**, 51-63.

Wettstein, D. A., Turner, D. L. and Kintner, C. (1997). The Xenopus homolog of Drosophila Suppressor of Hairless mediates Notch signaling during primary neurogenesis. *Development* **124**, 693-702.

Wilson, V. and Beddington, R. S. (1996). Cell fate and morphogenetic movement in the late mouse primitive streak. *Mech. Dev.* **55**, 79-89.

Yan, Y. L., Hatta, K., Riggleman, B. and Postlethwait, J. H. (1995). Expression of a type II collagen gene in the zebrafish embryonic axis. *Dev. Dyn.* **203**, 363-376.